ORIGINAL ARTICLE

Density mapping of nerve endings in the skin of the palm and flexor retinaculum of the hand. Application to open carpal tunnel release

Pedro Hernández-Cortés[1,2,3] | Patricia Hurtado-Olmo[1] | Olga Roda-Murillo[4] | Natividad Martín-Morales[5,6] | Francisco O'Valle[5,6]

[1]Upper Limb Surgery Unit, Orthopaedic Surgery Department, San Cecilio University Hospital of Granada, Granada, Spain

[2]Surgery Department, School of Medicine, Granada University, Granada, Spain

[3]Biosanitary Research Institut of Granada (IBS Granada), Granada, Spain

[4]Department of Human Anatomy, School of Medicine, Granada University, Granada, Spain

[5]Biomedical Research Centre of Granada (CIBM), Granada, Spain

[6]Pathology Department, School of Medicine, Granada University, Granada, Spain

Correspondence
Olga Roda-Murillo, Anatomy Department, School of Medicine of Granada, Avenida de la Investigación, 11. 18016 Granada, Spain.
Email: orroda@ugr.es

Abstract

In order to re-evaluate the safest area to incise skin and the flexor retinaculum (FR) when performing a carpal tunnel release (CTR), we carried out a mapping study of the nerve endings in the skin and FR on cadaver specimens, which, unlike previous studies for the first time, includes histomorphometry and image digital analysis. After dividing the skin and FR into 20 and 12 sections, respectively, we carried out a histomorphological analysis of nerve endings. The analysis was performed by two neutral observers on 4-μm histological sections stained with hematoxylin–eosin (H-E), and Klüver–Barrera with picrosirius red (KB+PR) methods. A semi-automatic image digital analysis was also used to estimate the percentage of area occupied per nerve. We observed a lower quantity of nerve endings in the skin of the palm of the hand in line with the ulnar aspect of the 4th finger. The ulnar aspect of the FR was the most densely innervated. However, there are no statistically significant differences between sections in the percentage of area occupied per nerve both in the skin and in the FR. We concluded that there is not a safe area to incise when performing carpal tunnel surgery, but taking into account the quantity of nerve endings present in skin and FR, we recommend an incision on the axis of the ulnar aspect of 4th finger when incising skin and on the middle third of the FR for CTR.

KEYWORDS
carpal tunnel release, carpal tunnel syndrome, cutaneous innervation, flexor retinaculum, hand, nerve ending, neuroma

1 | INTRODUCTION

Carpal tunnel syndrome (CTS) is a common condition affecting 1% of the population. The traditional surgical treatment of CTS involves the division of the flexor retinaculum (FR) to relieve pressure on the median nerve (Amadio, 2009; Kohanzadeh et al., 2012). This approach has long proven to be effective.

However, some patients experience postoperative complications derived from this operation, such as complex regional pain syndrome, postoperative scar tenderness, or pillar pain (Ludlow et al., 1997; Roux, 2004). All this contributes to both patient dissatisfaction and delay of their return to work (Boya et al., 2008; Huisstede et al., 2018).

The precise causes of these adverse events related to carpal tunnel release (CTR) remain unclear, but some authors have attributed them to injuries of the palmar cutaneous branch of the median and ulnar nerves, neurogenic inflammation, technical defects, or neuromas in the subcutaneous tissue (Biyani

et al., 1996; Ludlow et al., 1997; Monacelli et al., 2008; Tomaino & Plakseychuk, 1998).

Several authors have carried out different anatomical studies on the innervation of the palm of the hand to define a safe area to make the incision for open and endoscopic CTRs (Ozcanli et al., 2010; Samarakoon et al., 2014; Xu et al., 2013). Most studies are limited to the analysis of the macroscopic course of the palmar sensory branches of the median and ulnar nerves to define anatomical landmarks and, thus, avoid severing said structures (Hirtler et al., 2018; Martin et al., 1996; Smith & Ebraheim, 2019; Sulaiman et al., 2016; Tubbs et al., 2011).

It is widely accepted that the safest area to perform an open CTR is the cutaneous strip following the radial aspect of the 4th finger, proximal to the Kaplan line, that marks the location of the superficial palmar arch (Martin et al., 1996; Taleisnik, 1973; Watchmaker et al., 1996; Xu et al., 2013). Most hand surgeons accept this area as the safest to perform the incision, even though between 6% and 48% of patients who underwent open CTR experience pain in the heel of the palm (Boya et al., 2008; Huisstede et al., 2018; Monacelli et al., 2008).

When searching for a safe zone, we must consider not only the topography of macroscopic nerve structures, but also the microscopic density of nerve endings in the palm of the hand (Ruch et al., 1999). CTR involves both the skin incision and the division of the palmar fascia and the FR. This incision is particularly delicate as nerve structures might be injured due to variations in the sensory branch of the median nerve due to a transligamentous course (Ozcanli et al., 2010; Stecco et al., 2018).

In order to re-evaluate the safest area to make the skin incision and division of the FR when performing a CRT, we carried out a mapping study of the nerve endings in skin and FR on cadaveric specimens.

2 | METHODS

2.1 | Type of study

Basic anatomical and histomorphological research study of nerve endings density in the skin of the palm and FR in cadaveric specimens.

2.2 | Specimens

We used 10 forearm and hand specimens from seven fresh-frozen cadavers (4 males and 3 females) aged between 53 and 75 years at death, who had all given informed consent to their use for scientific purposes (McHanwell et al., 2008; Riederer et al., 2012).

The specimens had no previously documented wrist injuries or surgeries. All specimens were thawed at room temperature and dissected in the Human Anatomy Department of the School of Medicine of the University of Granada (Spain) between March and May 2020. Five right and five left forearm and hand specimens were studied.

Before in bloc extraction, the palm skin between the distal flexion crease of the wrist and the known "Kaplan line" (anatomical landmark that extends from the first web space to the hook of Hamate)

was divided and marked into 20 assessment sections to obtain a nerve density map after histomorphological analysis. Five longitudinal sections (A, B, C, D, and E) were drawn on the axis of the radial and ulnar aspects of the 3rd and 4th fingers and on the 4th-5th web space. Then, each section was subdivided into four identical sections from proximal to distal, numbered as shown in Figure 1a.

FR was harvested from the attachment of the scaphoid and trapezium bones in the radial side and at the border of ulnar neurovascular pedicle in the ulnar side. The specimen was also segmented into radial (A_{fr}), central (B_{fr}), and ulnar (C_{fr}) areas, and each one of them was, in turn, divided into four parts, two distal and two proximal, on both sides of the equatorial line (Figure 1b). This resulted in 12 areas numbered from 21 to 32.

2.3 | Histomorphological study

The samples of the different sections of the palmar skin and retinaculum were fixed in 10% buffered formalin for 48 h and then embedded in paraffin. Then, the 4-μm sections were proximal to distal longitudinally cut, dewaxed, and hydrated to stain with hematoxylin–eosin (H-E) and luxol fast blue plus picrosirius red methods, which were applied sequentially (Klüver–Barrera with picrosirius red staining, KB+PR). This double staining makes it possible to observe collagen fibres in red, myelin in blue, and the nucleus in a darkened color. The aim of said double staining is to increase the sensitivity of detection of nerve elements (Figure 2).

A millimeter scale in the eyepiece of a BH 2 microscope (Olympus Optical Company, Ltd.) with a 40× objective was used by two independent observers to count nerve structures in each strain. The results were expressed in terms of nerve endings/mm^2.

2.4 | Digital image analysis

To study the percentage of the area occupied by nerve structures, histomorphometry was performed semi-automatically on KB+PR-stained sections. For this purpose, we assessed 10 randomized images captured with a 10x objective through a microscope equipped with a digital camera DP70 (Olympus) connected to a computer and using the software ImageJ® v. 1.48 (NIH, USA, http://rsb.info.nih.gov/ij/). Separate quantifications of the total number of nerve structures and number of nerve structures per mm^2 were performed and expressed as area (mm^2) and percentage of each palmar and FR compartment (Figure 3).

2.5 | Statistical analysis

The statistical analyses were carried out through the SPSS software for Windows, version 23.0 (IBM SPSS Inc.). The normal distribution of quantitative variables was confirmed by Kolmogorov–Smirnov test. The number of nerve endings and the percentage of surface occupied per nerve are expressed through mean and standard
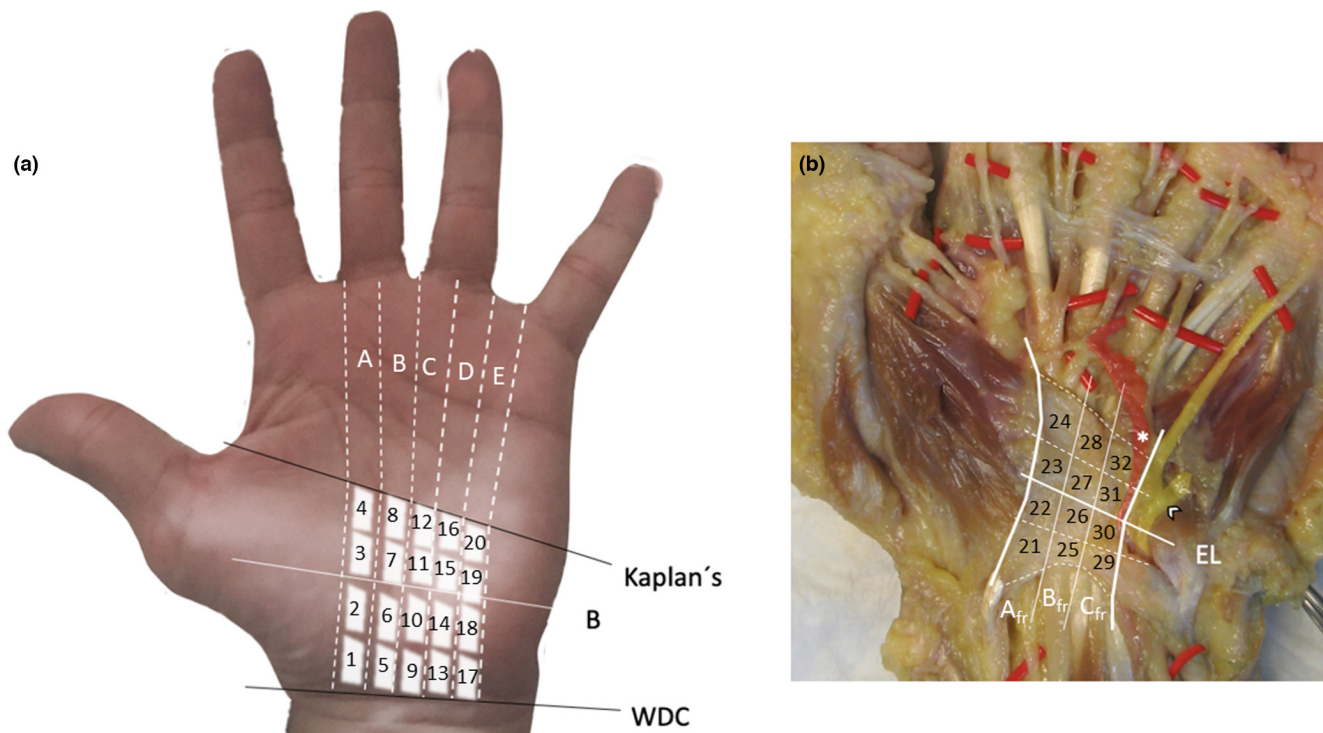
FIGURE 1 Diagram of the study areas in the skin (a) and in the flexor retinaculum (b)
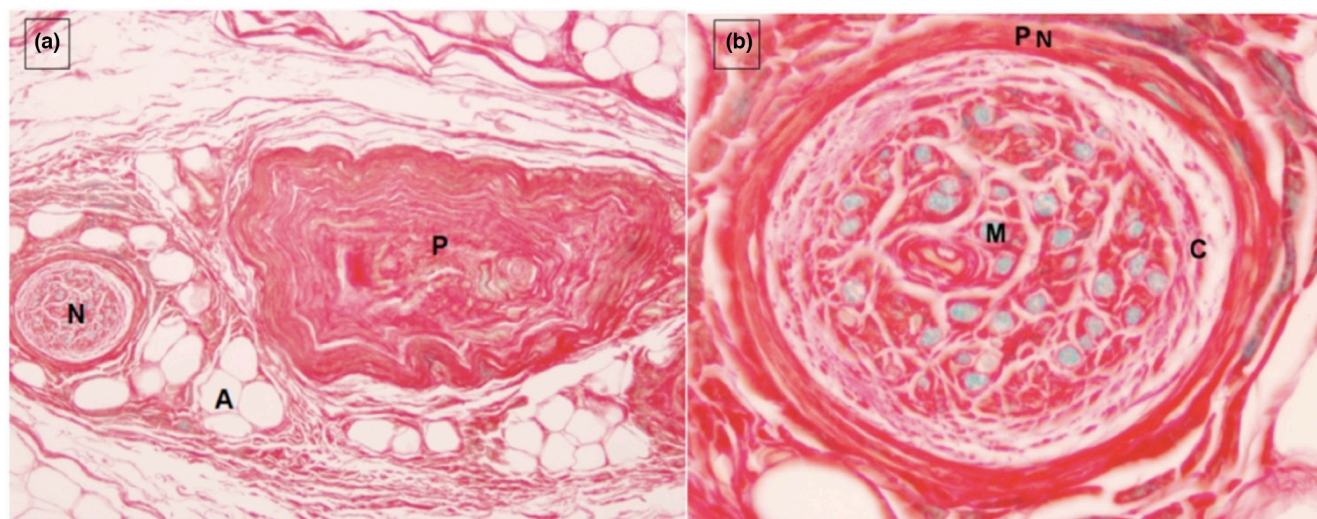

FIGURE 2 Klüver–Barrera with picrosirius red staining. This double staining makes it possible to observe collagen fibres in red, myelin in blue, and the nucleus in a darkened colour. (a) Vision of Paccini corpuscle. (b) Image of a crosss section of myelinated nerve. A, adipose tissue; C, connective tissue; M, myelin; N, nerve; P, paccini corpuscle; PN, perineurum

deviation. These variables were analyzed through the Student's *t*-test when comparing two sections and in case of independent samples or through the ANOVA test when comparing 3 or more sections.

To evaluate the reproducibility of the morphological study and the staining sensitivity of KB+PR, the level of concordance between the results of both staining analyses was established through an intra- and inter-observer comparison, which was made by means of Kendall's coefficient of concordance and Pearson's correlation coefficient. A confidence interval (CI) of 95% was considered significant (level $p < 0.05$).

3 | RESULTS

3.1 | Validity of −H-E staining methods against KB+PR staining and their reproducibility

The H-E and KB+PR staining methods allow to reliably assess the number of nerve structures and, although the number of nerves identified is higher with the modified KB+PR methods, the results were not statistically significant (Student's *t*-test; $p = 0.235$).
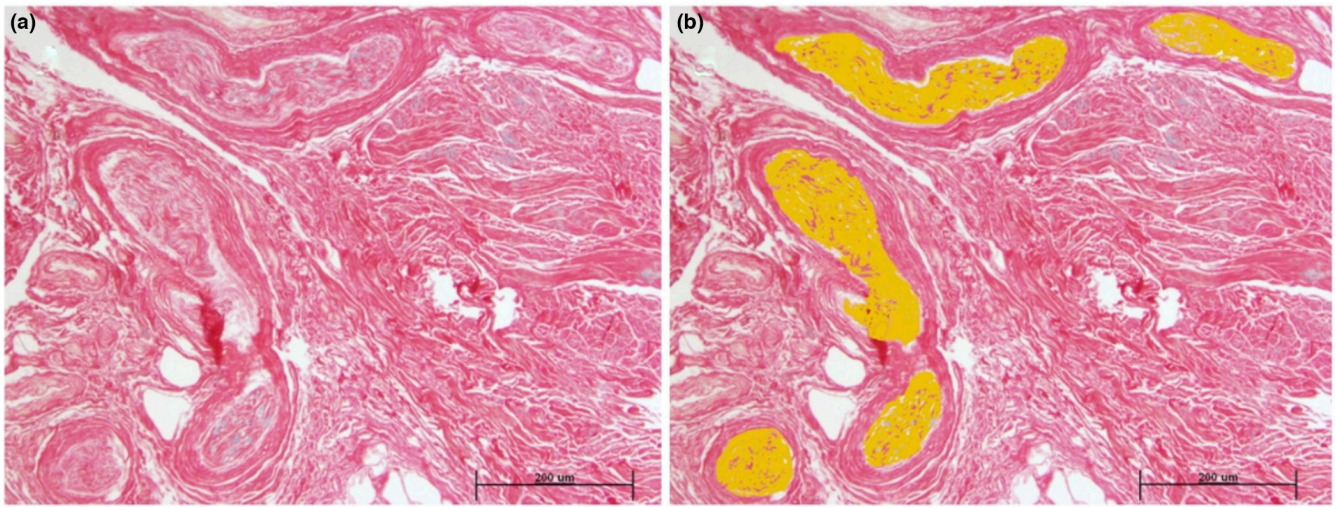
FIGURE 3 Images captured with a 10× objective through a microscope equipped with a digital camera DP70 (Olympus) connected to a computer and using the software ImageJ®. (a) Klüver–Barrera with picrosirius red staining. Histological section. (b) Umbralization procces of the nerve area
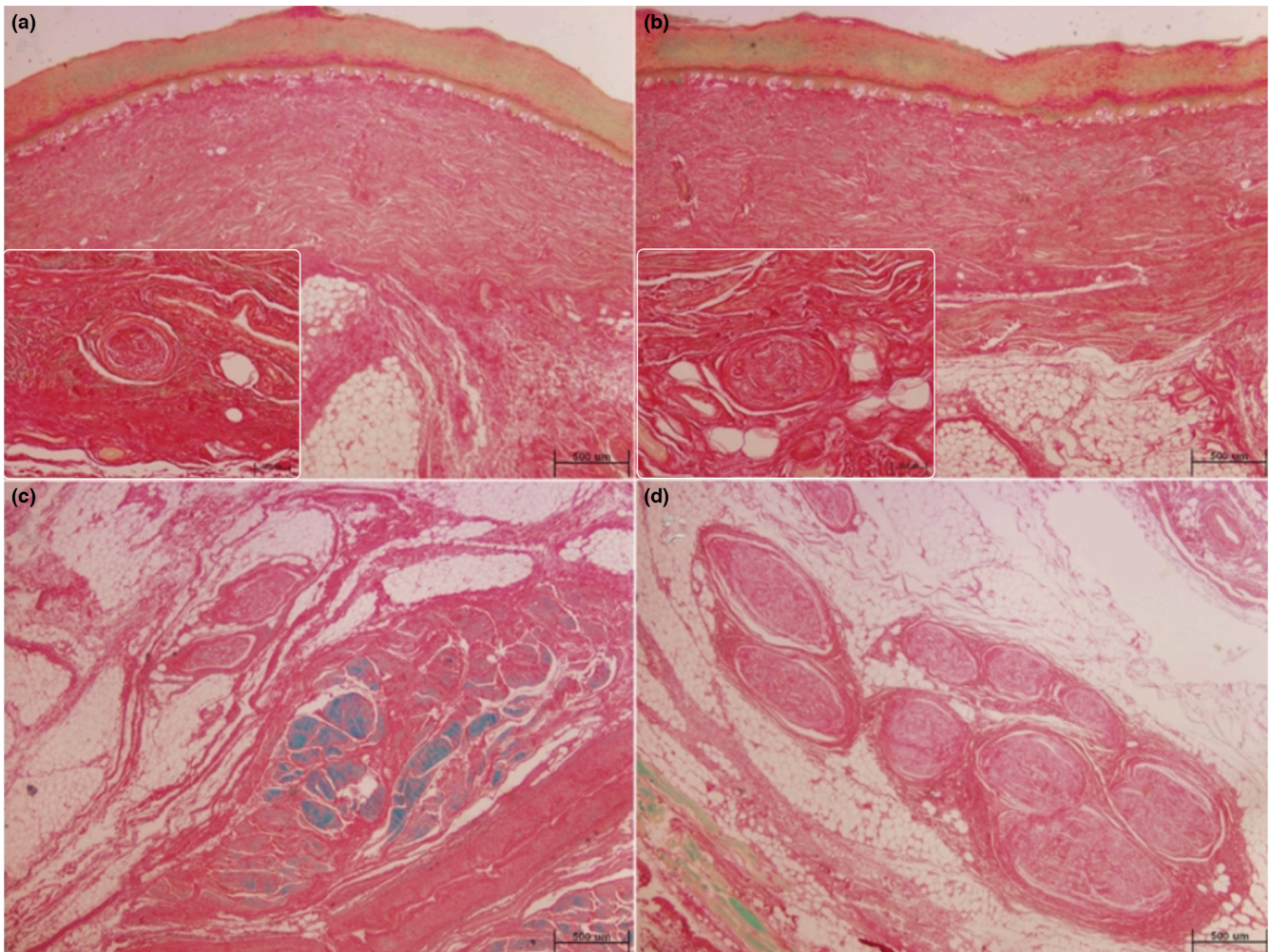
FIGURE 4 Histological images of Klüver–Barrera with picrosirius red stained skin and flexor retinaculum (FR tissue). (a, b) Correspond to areas 7 and 14 of the skin. Similarity can be seen in terms of sensitive nerve terminals that can be identified in the insert at 20×. (c, d) Correspond to areas 26 (central) and 30 (ulnar) of FR, respectively. The difference between the thickness of the nerve fascicles is clearly seen.

TABLE 1 Quantification of the number of nerve structures identified in the sections studied through both staining methods and according to each observer. Evaluation of 10 fields at 40× magnification and conversion into number of nerve elements per mm^2

Section	H-E observer 1	H-E observer 2	KB+PR observer 1	KB+PR observer 2	No. of nerves/mm^2 Total area
Palm of the hand #1	12.7	12±4.6	14.6±7.8	12±5.7	277.40±157.7
Palm of the hand #2	14±4.3	15.8±6.1	10±4.3	15.4±6.0	216.11±84.2
Palm of the hand #3	14.8±10.9	16.6±10.5	12.6±8.9	14.4±11.7	229.03±111.9
Palm of the hand #4	10.6±10.1	9.4±7.1	11.2±5.3	12±6.6	148.38±71.5
Palm of the hand #5	10.2±5.4	13±5.9	10.6±5.8	13.8±5.8	200.0±99.8
Palm of the hand #6	13±14.1	11.2±7.2	7.2±3.9	11.2±7.4	132.25±79.3
Palm of the hand #7	10.8±8.4	12.6±7.1	8.2±5.7	13.8±5.3	174.19±97.0
Palm of the hand #8	10.2±3.9	10±5.7	8.0±6.1	12.8±5.2	164.51±95.0
Palm of the hand #9	7.4±3.5	9.0±4.2	9.4±5.9	8.0±4.7	158.06±71.5
Palm of the hand #10	8.8±6.5	11.6±7.4	11.6±6.7	14.8±8.1	193.54±148.2
Palm of the hand #11	10.4±6.4	10.2±5.5	7.6±5.4	9.8±6.2	174.19±123.0
Palm of the hand #12	19.6±25.6	10.0±10.9	16.2±21.9	10.0±11.8	293.54±423.5
Palm of the hand #13	9.6±3.7	10.4±5.2	7.4±5.4	8.2±5.8	193.54±67.4
Palm of the hand #14	6.2±4.1	7.6±4.3	9.2±7.9	9.8±5.4	145.15±57.0
Palm of the hand #15	11.4±4.3	11.8±6.1	6.8±5.7	10±6.3	129.03±106.3
Palm of the hand #16	8.0±5.9	8.4±4.5	9.0±5.5	8.6±5.5	148.38±115.4
Palm of the hand #17	6.8±7.0	7.8±7.1	9.8±8.7	11.2±8.8	183.87±200.3
Palm of the hand #18	12.8±11.1	12.8±9.5	8.2±3.8	16.8±15.4	229.03±126.6
Palm of the hand #19	10.2±3.1	12.4±4.8	11.8±9.9	13.6±9.9	190.32±108.4
Palm of the hand #20	13.8±6.8	12.2±5.7	10.6±4.6	10.2±2.6	193.54±103.9
FR #21	1.8±2.1	1.6±2.6	3.8±3.2	5.0±6.2	38.71±35.3
FR #22	6.4±5.8	6.0±5.9	6.8±5.7	10.6±7.16	106.45±60.9
FR #23	2.4±3.2	2.4±2.7	3.6±2.9	2.8±2.6	29.03±33.0
FR #24	2.4±2.8	2±2.5	3.8±6.4	4.0±4.7	29.03±47.5
FR #25	5.0±3.3	6.2±4.0	6.0±6.0	6.6±7.6	41.93±55.4
FR #26	4.4±5.5	5.2±9.4	3.2±3.8	7.2±7.2	22.58±24.4
FR #27	2.6±3.2	3.6±3.7	3.6±3.5	3.6±4.2	16.13±27.9
FR #28	3.4±4.3	5.8±2.9	3.6±5.1	6.0±5.2	32.25±34.2
FR #29	8.4±4.2	9.0±6.1	6.4±3.2	12.2±10.6	90.32±81.9
FR #30	5.2±4.0	4.8±4.5	2.8±3.0	7.4±7.6	64.51±27.4
FR #31	4.0±3.0	5.4±4.9	1.4±2.0	4.2±4.0	38.71±37.1
FR #32	7.0±6.7	9.2±9.0	6.2±7.2	10.8±10.1	116.12±121.1

Note: H-E Observer 1: Count of nerve fibres in sections stained with hematoxylin-eosin, performed by observer 1. H-E Observer 2: Count of nerve fibres in sections stained with hematoxylin-eosin, performed by observer 2. KB+PR Observer 1: Count of nerve fibres in sections stained with Klüver-Barrera+picrosirius red, performed by observer 1. KB+PR Observer 2: Count of nerve fibres in sections stained with Klüver-Barrera+picrosirius red, performed by observer 2. No. of nerves/mm^2. Total area: Count of nerve fibres per mm^2 identified through KB+PR. Mean of both observers.

Abbreviation: FR, flexor retinaculum.

The Kendall's coefficient of concordance of the results obtained by the two independent observers was good/moderate when the nerve structures were evaluated with H-E (Kendall's coefficient of concordance 0.669, $p =<0.001$) and somewhat weaker when they were evaluated with the modified KB+PR staining (Kendall's coefficient of concordance 0.464; $p <0.001$).

There is a high statistical correlation for both staining methods between the results obtained by the two observers, with the highest values between the two stainings being those obtained by observer 2 (Pearson's correlation coefficient $r = 0.832$; $p = 0.000$).

3.2 | Distribution of nerve endings in skin and FR

The nerve structures in the FR are larger than in the skin, particularly in the ulnar area. The innervation of the palm of the hand shows a

greater number of medium or small calibre nerves surrounded by a dense connective tissue of the perineurium, as evidenced by the KB+PR staining method designed for this study (Figures 3 and 4).

Table 1 presents the mean and dispersion values of the nerve structures obtained in the different sections analyzed through both staining methods.

The mean of nerve endings (n/mm^2) was lower in the FR (sections 21–32) than in the palm skin (sections 1–20), regardless of the staining method used to evaluate them. Table 2 presents a comparison between nerve density of the skin of the palm and of the FR (Student's t-test; $p < 0.005$, $p < 0.011$, $p < 0.001$).

3.3 | Quantity of nerve endings in the skin of the palm

No statistically significant differences were observed when comparing proximal and distal sections of the skin of the palm, regardless of the staining used for analysis (Student's t-test; $p = 0.620$, $p = 0.774$, $p = 0.665$) (Table 3). However, there were significant differences between the longitudinal sections (one-way ANOVA; $p < 0.001$), with band D having a lower count of nerve endings compared with band A (Bonferroni correction; $p < 0.001$), (Table 4; Figures 4 and 5).

3.4 | Quantity of nerve endings in the FR

We observed a greater number of nerve elements in the proximal section of the FR than in its distal zone, but the difference was not statistically significant (Student's t-test; $p = 0.251$, $p = 0.750$, $p = 0.731$, respectively), (Table 5; Figures 4 and 5).

When comparing longitudinal sections, we found a statistically significant higher nerve density in the ulnar portion of the FR than in its central and radial portions (one-way ANOVA; $p = 0.014$), (Table 6; Figure 4).

3.5 | Digital image analysis of the area occupied by nerve structures

Table 7 presents the percentage of area (mm^2) occupied per nerve in the different sections studied. They are represented in a color spectrum diagram in Figure 6. The area occupied per nerve is significantly greater in the FR than in the skin of the palm (Student's t-test; $p < 0.001$).

Regarding the skin of the palm, there were no statistically significant differences in the area occupied per nerve between the distal and proximal sections (Student's t- test; $p = 0.442$), nor between the different longitudinal bands (one-way ANOVA; $p = 0.564$).

TABLE 2 Statistical study of the comparison between nerve density of the skin of the palm and of the FR. Comparison between nerve density of the skin of the palm (sections 1–20) and of the tissue of the FR (sections 21–32). Statistical comparison by means of Student's t-test. p Values are shown in the right column of the table (significance level).

	Variables	Mean	Standard deviation	Student's t-test p Values
Total nerve count (H-E)	Palm of the hand	11.07	9.04	0.005
	FR	4.42	4.34	
Total nerve count (KB+PR)	Palm of the hand	10.00	7.56	0.011
	FR	4.27	4.51	
No. of nerves/mm^2 (all fields)	Palm of the hand	188.70	136.83	0.001
	FR	52.15	61.96	

Abbreviations: FR, flexor retinaculum; H-E, hematoxylin–eosin; KB+PR, Klüver–Barrera with picrosirius red.

TABLE 3 Comparison between number of nerve elements found per mm^2 of skin of the palm of the hand (10 fields at 40×). Proximal portions (sections 1, 2, 5, 6, 9, 10, 13, 14, 17, and 18) are compared against distal portions (sections 3, 4, 7, 8, 11, 12, 15, 16, 19, and 20).

	Variables	Mean	Standard deviation	Student's t-test p Values
Count (10 fields at 40×) hematoxylin–eosin	Proximal	10.70	6.44	0.620
	Distal	11.78	6.62	
Count (10 fields at 40×) Klüver-Barrera+picrosirius red	Proximal	11.78	7.81	0.774
	Distal	11.86	7.15	
No. of nerves/mm^2	Proximal	186.13	116.5	0.665
	Distal	191.29	155.69	

TABLE 4 Statistical study of comparison between the number of nerve elements found in the different longitudinal bands (A, B, C, D, and E) of the skin of the palm of the hand (10 fields at 40×; mean count of H-E and KB+PR stainings)
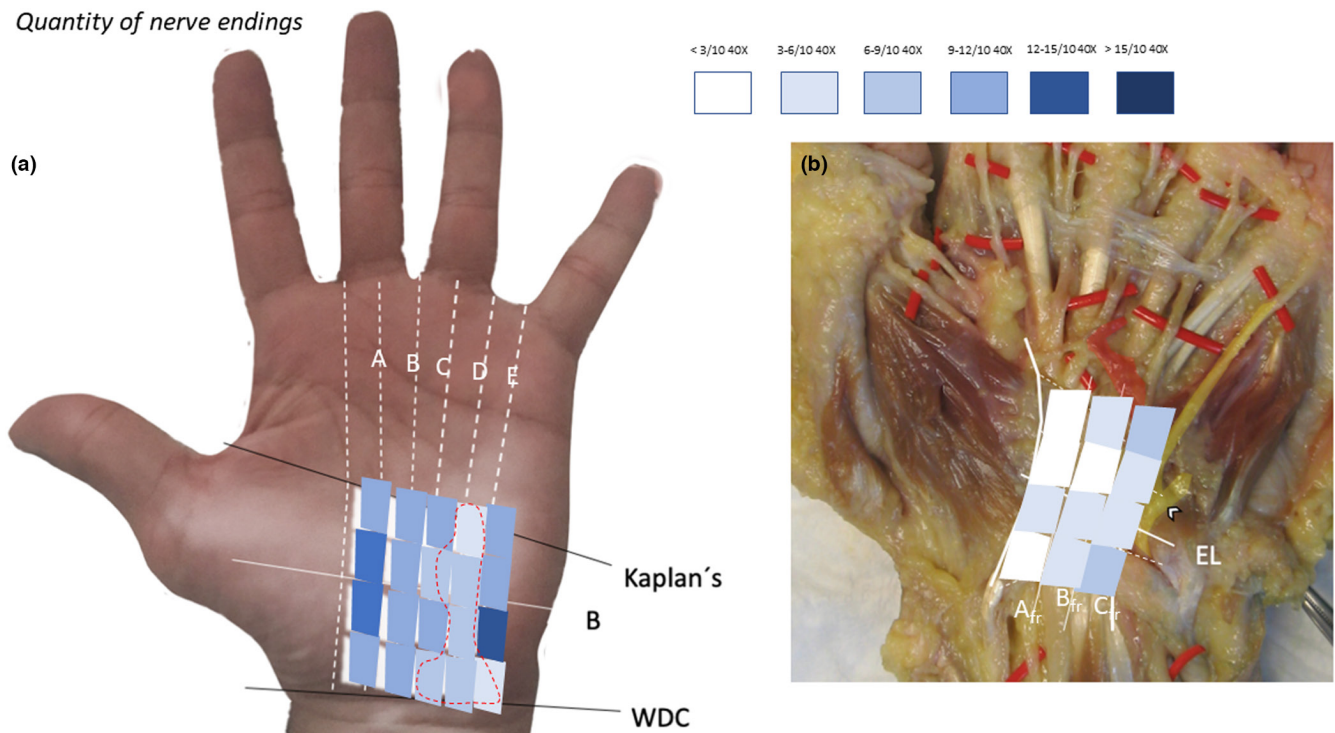
Section	Mean	Standard deviation	Statistical formula
A	13.04	2.13	ANOVA $p < 0.001$
B	11.03	2.05	
C	10.90	3.32	
D	8.90	1.56	
E	11.31	2.52	

Post hoc analysis (Bonferroni correction)					
	A	**B**	**C**	**D**	**E**
A		$p = 0.204$	$p = 0.134$	$p < 0.001$	$p = 0.443$
B	$p = 0.204$		$p = 1.0$	$p = 0.137$	$p = 1.0$
C	$p = 0.134$	$p = 1.0$		$p = 0.207$	$p = 1.0$
D	$p < 0.001$	$p = 0.137$	$p = 0.207$		$p = 0.056$
E	$p = 0.443$	$p = 1.0$	$p = 1.0$	$p = 0.056$	

Abbreviations: H-E, hematoxylin–eosin; KB+PR, Klüver–Barrera with picrosirius red.

FIGURE 5 Color diagram density map of the skin (a) and flexor retinaculum (b) based in number of nerve endings count. Red dashed line marks the area corresponding to lesser innervation density and where we propose to localize the incision for carpal tunnel release

Similarly, there were no statistically significant differences in the area occupied per nerve between the distal and proximal portions of the FR (Student's t-test; $p = 0.857$), nor between longitudinal sections (one-way ANOVA; $p = 0.257$).

4 | DISCUSSION

This article presents a study on nerve density of the skin of the palm and FR including histomorphometry and image digital analysis, with the aim of providing results that can be applied to carpal tunnel syndrome surgery. The results show that the areas with fewer nerve elements are the skin band in the axis of the ulnar aspect of 4th finger of the hand and the central part of the FR. However, there were no differences in the percentage of area occupied per nerve between the skin areas, and the FR.

Most studies on nerve mapping of the palm of the hand are limited to gross dissection of sensitive branches of the median and ulnar nerves (Bezerra et al., 1986; Born & Mahoney, 1995; Hobbs et al., 1990; Martin et al., 1996; Matloub et al., 1998; Natsis

et al., 2012; Ozcanli et al., 2010; Sulaiman et al., 2015; Tubbs et al., 2011) and conclude that the safest area to make a skin incision is the one proximal to the superficial arterial arch of the hand in the axis of the radial aspect of the 4th finger. This surgical approach, suggested by Tailesnik in 1973, has become the gold standard when performing carpal tunnel syndrome surgery.

As far as we know, Ruch et al. (1999) are the only ones who have performed a histomorphometric study of 4-μm sections stained with H-E to map the nerve density of the skin of the palm and underlying tissues. According to them, the safest area (with the lowest nerve density) would be the gap between the axes of the third and fourth metacarpal bones, 2 cm proximal to the Kaplan line. Said authors also stated that the FR is a structure relatively devoid of nerves and that its incision is not likely to form a neuroma or lead to postoperative pain.

We present a similar study, but with a greater subdivision of skin sections, including an additional ulnar section. Besides, we sequentially used two staining methods—luxol fast blue and picrosirius red staining—not previously considered for this purpose. This double staining allowed us to better identify the myelinated nerve structures in both the dermal connective tissue of the skin and the FR, which become blue stained (as myelin) when only the Klüver–Barrera staining method is applied. When performing the picrosirius red staining method, the dermal connective tissue of the skin

and the FR get red stained, thus enabling the identification of the perineurium and epineurium, and staining green the epithelium and vascular structures. This green staining prevents the epitelium and vascular structures from leading to error, as often happens when other staining methods are used.

With this combined technique, it was possible to identify more nerve structures, but not in a statistically significant way. Additionally, correlations for both staining methods and between the results obtained by both observers were high, so this modification is considered suitable for the histomorphometric study of nerve endings.

We have no record of any other nerve mapping study of the palm of the hand where image digital analysis was used. However, its efficacy and reproducibility regarding the identification of nerve elements in the skin have been already demonstrated, regardless of the
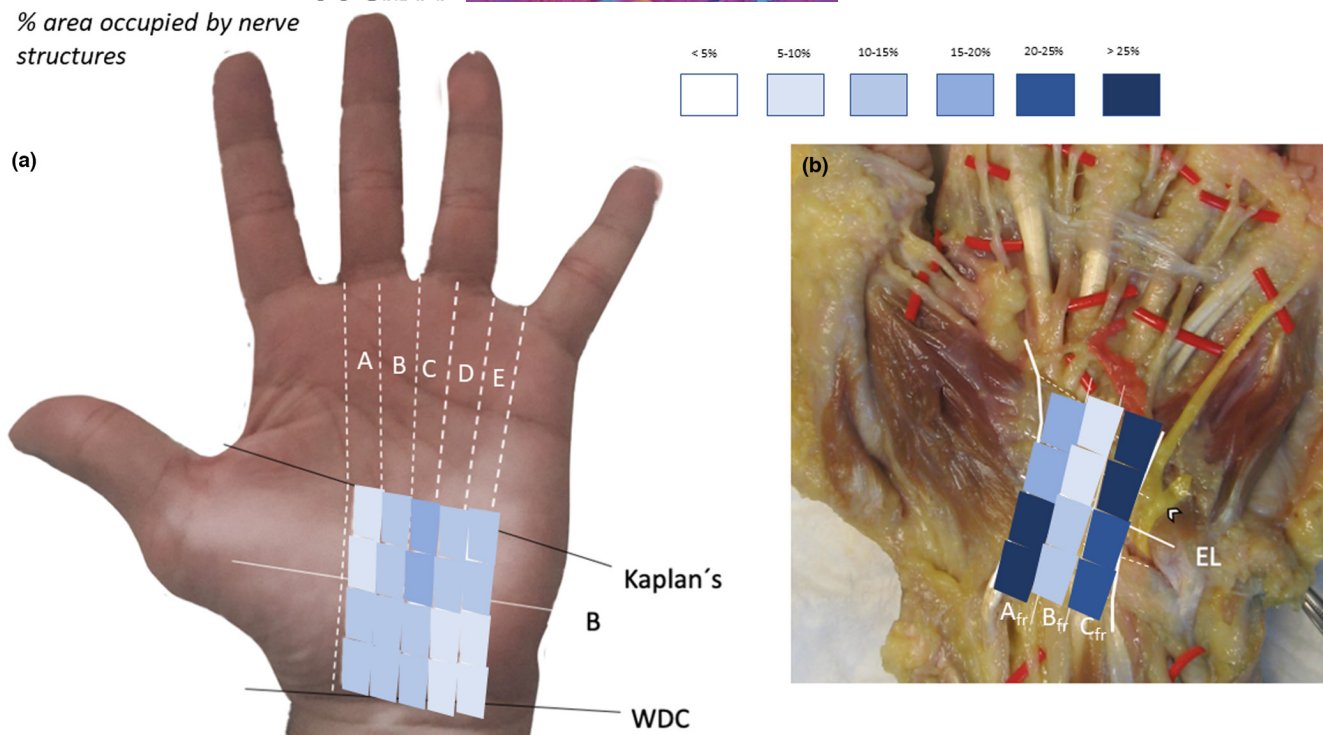
TABLE 5 Comparison of the number of nerve elements per mm^2 between the proximal portion (sections 21, 22, 25, 26, 29, and 30) and the distal portion (sections 23, 24, 27, 28, 31, and 32) of the FR (10 fields at 40×)

	Variables	Mean	Standard deviation	ANOVA test p Values
Total count (H-E)	FR, proximal	5.20	4,48	0.251
	FR, distal	3.63	4.12	
Total count (KB+PR)	FR, proximal	4.83	4,29	0.750
	FR, distal	3.70	4,72	
No. of nerves/ mm^2	FR, proximal	60.752	59.55	0.731
	FR, distal	43.55	64.12	

Abbreviations: FR, flexor retinaculum; H-E, hematoxylin–eosin; KB+PR, Klüver–Barrera with picrosirius red.

TABLE 7 Percentage of area occupied per nerve in the different sections studied

	Sections	Mean	Standard deviation
Skin of the palm of the hand	1–2	10.48	4.19
	3–4	9.69	6.10
	5–6	13.68	10.08
	7–8	9.80	3.46
	9–10	11.91	4.53
	11–12	15.17	12.72
	13–14	7.20	3.57
	15–16	10.39	4.71
	17–18	7.96	3.64
	19–20	13.31	6.40
FR	21–22	27.28	32.84
	23–24	16.20	15.27
	25–26	10.55	13.22
	27–28	6.05	4.71
	29–30	21.13	36.46
	31–32	31.61	34.11
Comparison palm versus FR	Student's t-test; $p < 0.001$		

Abbreviation: FR, flexor retinaculum.

TABLE 6 Statistical study of the comparison between the number of nerve elements in the different longitudinal sections (A$_{fr}$, B$_{fr}$, C$_{fr}$) of the FR (10 fields at 40×)

	Mean	Standard deviation	ANOVA	Sum of the squares	df	Root mean square	F	Significance level (Bonferroni correction)
A$_{fr}$	4.08	2.39	Among groups	50.832	2	25.416	4.715	Section A$_{fr}$ against section B$_{fr}$: $p = 1.0$.
B$_{fr}$	4.75	1.42	Within groups	242.587	45	5.391		Section A$_{fr}$ against C$_{fr}$: $p = 0.014$.
C$_{fr}$	6.52	2.90	Total	293.419	47			Section B$_{fr}$ against section C$_{fr}$: $p = 0.108$.
ANOVA; $p = 0.014$								

FIGURE 6 Color diagram density map of the skin (a) and flexor retinaculum (FR) (b) based in percentage of the area occupied by nerve structures. The ulnar border of the FR must be avoided when opening carpal tunnel

experience of the researcher involved (Provitera et al., 2015; Seger et al., 2016). In our case, this tool solved a problem regarding the size of the nerve endings, which was already pointed out by Ruch et al. (1999). Like the previously mentioned authors, we observed that the nerve elements found in the sections with a lower count had a greater diameter than those found in sections with a higher count. Using image digital analysis allowed us to semi-automatically estimate the percentage of area occupied by the nerve, which, in our opinion, better indicates nerve density.

Many authors intend to define an internervous plane between the median and ulnar nerves to use it in CTR with the assumption that the border area between the course of two nerves is a low nerve endings density zone. Based in macroscopic dissection studies they suggest several incisions: in the axis on the radial aspect of the 4th finger (Taleisnik, 1973); immediately ulnar and parallel to the thenar crease, in the axis on the ulnar aspect of the 4th finger (Gelberman & North, 1991); in the axis on the ulnar aspect of the 4th finger (Eversmann, 1993); 5 mm ulnar to the crease between thenar and hypothenar eminences (Watchmaker et al., 1996); in projection with the 3rd commissural area (Boughton et al., 2010); and in a 5 mm band on both sides of the axis of the 3rd finger (Xu et al., 2013).

Even when these incisions are made, persistent postoperative scar tenderness (incidence ranges from 19% to 61%) (Kluge et al., 1996; Monacelli et al., 2008), and the most feared pillar pain (Ludlow et al., 1997) could be experienced. Numerous variants and nerve networks justify an overlapping of the nerve supply areas of median and ulnar nerves (Biafora & Gonzalez, 2007; Ferrari & Gilbert, 1991; Natsis et al., 2012; Sulaiman et al., 2015; Unver Dogan

et al., 2010) and some authors reject the assertion that there is an area of lower nerve density (Ozcanli et al., 2010). In a dissection study on 24 cadaver specimens and by means of the Tailesnik's incisions, Born and Mahoney (1995) found part of the course of the cutaneous sensory branch of the ulnar nerve in 12% of cases and of the palmar cutaneous branch of the median nerve in 8% of cases in vicinity of the incision. Wheatley et al. (1996) took random intraoperative biopsies from the wounds of 15 patients who underwent a CTR and found nerve elements in the tissue in all cases.

In such circumstances, minimal incision interventions or endoscopic release of the carpal tunnel seem to be the only reasonable alternatives. However, although they decrease the postoperative scar tenderness and pillar pain rates and enable an earlier return to work, they do not completely avoid the pain in the heel of the palm (Ludlow et al., 1997; Teng et al., 2019).

This fact may lead one to think that cutaneous innervation is not the only cause of postoperative pain in the heel of the hand and other deeper tissues should be considered in this regard. When the proximal portion of the retinaculum is cut and scissors are pushed under the skin to open the antebrachial fascia, palmar cutaneous branches of the ulnar and median nerves cannot be seen and are left at risk for injury.

Stecco et al. (2018) show the high innervation of palmar aponeurosis in a histomorphometric study on biopsies from patients treated for Dupuytren's contracture. Although some authors maintain that the FR is practically devoid of nerve structures (Ruch et al., 1999; Stecco et al., 2018), in our study we invariably observed the continuous presence of nerve elements with a higher calibre than the nerve endings

of the palmar skin. Image digital analysis was especially useful in this regard. A nerve injury in this area may cause pain in the heel of the hand, even when there is no incision in the skin. Besides, we have observed and proven that there is a statistically significant higher nerve density in the ulnar aspect of the FR in comparison with its middle and radial portions. Indeed, most hand surgeons open the FR through its most ulnar aspect to avoid the median nerve and protect it from the resulting scar. According to the results obtained in the present study, the mentioned incision made in the FR should be rectified.

The main constraint present in this study is the small size of the sample evaluated. Additionally, the relative location of the cutaneous strips may be altered by the loss of tissue muscle tone of the cryo-preserved cadaver. On the other hand, this paper presents a double staining study, double-blind evaluation of the counting of nerve endings with a high correlation rate and the addition of the determination of the area occupied per nerve through a digital semi-automatic tool.

In conclusion, the percentage of area occupied per nerve is quite homogeneous, with no differences between areas of skin and FR and, thus, there is no safe area to make the incision. Quantitatively, the present study shows that there is an area with fewer nerve endings than the average, which is in the skin of the palm of the hand, adjacent to the ulnar aspect of the 4th finger. We consider this area suitable for the CTR incision. At the same time, more nerve elements than the average are found in the ulnar border of the FR, which is the reason why we also recommend dividing such structure into its central portions.

AUTHOR CONTRIBUTIONS

All authors contributed to the study conception. PHC and FO were responsible of the design. Material preparation and in block extraction of the tissue samples were performed by OR, PHC, and PHO. Data base was done by PHO and NMM. Statistical analysis were done by PHC. The count of the nervous structures on the histological sections stained with H–E and Kluver–Barrera combined with sirio red was performed by PHO and FO. Digital image analysis was carried out by NMM. The first draft of the manuscript was written by PHC, FO, and OR and all authors commented on previous versions of the manuscript. All authors read and approved the final manuscript.

ACKNOWLEDGMENTS

DATA AVAILABILITY STATEMENT

We have not shared any data. We have no problem that the data is shared from now on.

ORCID

Olga Roda-Murillo https://orcid.org/0000-0001-8696-6313

REFERENCES

Amadio, P.C. (2009) Interventions for recurrent/persistent carpal tunnel syndrome after carpal tunnel release. *Journal of Hand Surgery*, 34(7), 1320–1322.

Bezerra, A.J., Carvalho, V.C. & Nucci, A. (1986) An anatomical study of the palmar cutaneous branch of the median nerve. *Surgical and Radiologic Anatomy*, 8(3), 183–188.

Biafora, S.J. & Gonzalez, M.H. (2007) Sensory communication of the median and ulnar nerves in the palm. *Journal of Surgical Orthopaedic Advances*, 16(4), 192–195.

Biyani, A., Wolfe, K., Simison, A.J. & Zakhour, H.D. (1996) Distribution of nerve fibers in the standard incision for carpal tunnel decompression. *Journal of Hand Surgery*, 21, 855–857.

Born, T. & Mahoney, J. (1995) Cutaneous distribution of the ulnar nerve in the palm: does it cross the incision used in carpal tunnel release? *Annals of Plastic Surgery*, 35(1), 23–25.

Boughton, O., Adds, P.J. & Jayasinghe, J.A. (2010) The potential complications of open carpal tunnel release surgery to the ulnar neurovascular bundle and its branches: a cadaveric study. *Clinical Anatomy*, 23(5), 545–551.

Boya, H., Ozcan, O. & Oztekin, H.H. (2008) Long-term complications of open carpal tunnel release. *Muscle & Nerve*, 38, 1443–1446.

Eversmann, W.W., Jr. (1993) Entrapment and compression neuropathies. In: Green, D.P. (Ed.) *Operative hand surgery*, 3rd edition. New York: Churchill Livingstone, pp. 1341–1385.

Ferrari, G.P. & Gilbert, A. (1991) The superficial anastomosis on the palm of the hand between the ulnar and median nerves. *Journal of Hand Surgery: British & European Volume*, 16(5), 511–514.

Gelberman, R.H. & North, E.R. (1991) Open carpal tunnel release. In: Gelberman, R.H. (Ed.) *Operative nerve repair and reconstruction*. Philadelphia: JP Lippincott, pp. 899–913.

Hirtler, L., Huber, F.A. & Wlodek, V. (2018) Cutaneous innervation of the distal forearm and hand—minimizing complication rate by defining danger zones for surgical approaches. *Annals of Anatomy*, 220, 38–50.

Hobbs, R.A., Magnussen, P.A. & Tonkin, M.A. (1990) Palmar cutaneous branch of the median nerve. *The Journal of Hand Surgery*, 15(1), 38–43.

Huisstede, B.M., van den Brink, J., Randsdorp, M.S., Geelen, S.J. & Koes, B.W. (2018) Effectiveness of surgical and postsurgical interventions for carpal tunnel syndrome—a systematic review. *Archives of Physical Medicine and Rehabilitation*, 99, 1660–1680.

Kluge, W., Simpson, R.G. & Nicol, A.C. (1996) Late complications after open carpal tunnel decompression. *Journal of Hand Surgery*, 21(2), 205–207.

Kohanzadeh, S., Herrera, F.A. & Dobke, M. (2012) Outcomes of open and endoscopic carpal tunnel release: a meta-analysis. *Hand*, 7(3), 247–245.

Ludlow, K.S., Merla, J.L., Cox, J.A. & Hurst, L.N. (1997) Pillar pain as a postoperative complication of carpal tunnel release: a review of the literature. *Journal of Hand Therapy*, 10(4), 277–282.

Martin, C.H., Seiler, J.G., 3rd & Lesesne, J.S. (1996) The cutaneous innervation of the palm: an anatomic study of the ulnar and median nerves. *Journal of Hand Surgery*, 21(4), 634–638.

Matloub, H.S., Yan, J.G., Mink Van Der Molen, A.B., Zhang, L.L. & Sanger, J.R. (1998) The detailed anatomy of the palmar cutaneous nerves and its clinical implications. *Journal of Hand Surgery: British & European Volume*, 23(3), 373–379.

McHanwell, S., Brenner, E., Chirculescu, A.R.M., Drukker, J., van Mameren, H., Mazzotti, G. et al. (2008) The legal and ethical framework governing body donation in Europe—a review of current practice and recommendations for good practice. *European Journal of Anatomy*, 12, 1–24.

Monacelli, G., Rizzo, M.I., Spagnoli, A.M., Pardi, M. & Irace, S. (2008) The pillar pain in the carpal tunnel's surgery. Neurogenic inflammation? A new therapeutic approach with local anaesthetic. *Journal of Neurosurgical Sciences*, 52(1), 11–15.

Natsis, K., Karanassos, M.T., Papathanasiou, E. & Noussios, G. (2012) A coexisting anatomical variation of median and ulnar nerves in a cadaver palm. *Folia Morphologica*, 71(4), 269–274.

Ozcanli, H., Coskun, N.K., Cengiz, M., Oguz, N. & Sindel, M. (2010) Definition of a safe-zone in open carpal tunnel surgery: a cadaver study. *Surgical and Radiologic Anatomy*, 32(3), 203–206.

Provitera, V., Nolano, M., Stancanelli, A., Caporaso, G., Vitale, D.F. & Santoro, L. (2015) Intraepidermal nerve fiber analysis using immunofluorescence with and without confocal microscopy. *Muscle & Nerve*, 51(4), 501–504.

Riederer, B.M., Bolt, S., Brenner, E., Bueno-López, J.L., Circulescu, A.R.M., Davies, D.C. et al. (2012) The legal and ethical framework governing body donation in Europe-1st update on current practice. *European Journal of Anatomy*, 16, 1–21.

Roux, J.L. (2004) Treatment of the post-surgical complications of carpal tunnel syndrome. *Chirurgie de la Main*, 23(Suppl. 1), 178–187.

Ruch, D.S., Marr, A., Holden, M., James, P., Challa, V. & Smith, B.P. (1999) Innervation density of the base of the palm. *Journal of Hand Surgery*, 24(2), 392–397.

Samarakoon, L.B., Guruge, M.H., Jayasekara, M., Malalasekera, A.P., Anthony, D.J. & Jayasekara, R.W. (2014) Anatomical landmarks for safer carpal tunnel decompression: an experimental cadaveric study. *Patient Safety in Surgery*, 8(1), 8.

Seger, S., Stritt, M., Doppler, K., Frank, S., Panaite, A., Kuntzer, T. et al. (2016) A semi-automated method to assess intraepidermal nerve fibre density in human skin biopsies. *Histopathology*, 68(5), 657–665.

Smith, J.L. & Ebraheim, N.A. (2019) Anatomy of the palmar cutaneous branch of the median nerve: a review. *Journal of Orthopaedics*, 16(6), 576–579.

Stecco, C., Macchi, V., Barbieri, A., Tiengo, C., Porzionato, A. & De Caro, R. (2018) Hand fasciae innervation: the palmar aponeurosis. *Clinical Anatomy*, 31(5), 677–683.

Sulaiman, S., Soames, R. & Lamb, C. (2015) Ulnar nerve cutaneous distribution in the palm: application to surgery of the hand. *Clinical Anatomy*, 28(8), 1022–1028.

Sulaiman, S., Soames, R. & Lamb, C. (2016) An anatomical study of the superficial palmar communicating branch between the median and ulnar nerves. *Journal of Hand Surgery (European Volume)*, 41(2), 191–197.

Taleisnik, J. (1973) The palmar cutaneous branch of the median nerve and the approach to the carpal tunnel. An anatomical study. *Journal of Bone and Joint Surgery*, 55(6), 1212–1217.

Teng, X., Xu, J., Yuan, H., He, X. & Chen, H. (2019) Comparison of wrist arthroscopy, small incision surgery, and conventional surgery for the treatment of carpal tunnel syndrome: a retrospective study at a single center. *Medical Science Monitor*, 25, 4122–4129.

Tomaino, M.M. & Plakseychuk, A. (1998) Identification and preservation of palmar cutaneous nerves during open carpal tunnel release. *Journal of Hand Surgery: British & European Volume*, 23, 607–608.

Tubbs, R.S., Rogers, J.M., Loukas, M., Cömert, A., Shoja, M.M. & Cohen-Gadol, A.A. (2011) Anatomy of the palmar branch of the ulnar nerve: application to ulnar and median nerve decompressive surgery. *Journal of Neurosurgery*, 114(1), 263–267.

Unver Dogan, N., Uysal, I.I., Karabulut, A.K., Seker, M. & Ziylan, T. (2010) Communications between the palmar digital branches of the median and ulnar nerves: a study in human fetuses and a review of the literature. *Clinical Anatomy*, 23(2), 234–241.

Watchmaker, G.P., Weber, D. & Mackinnon, S.E. (1996) Avoidance of transection of the palmar cutaneous branch of the median nerve in carpal tunnel release. *Journal of Hand Surgery*, 21(4), 644–650.

Wheatley, M.J., Hall, J.W. & Faringer, P.D. (1996) Are the palmar cutaneous nerves safe during standard carpal tunnel release? *Annals of Plastic Surgery*, 37(3), 251–253.

Xu, X., Lao, J. & Zhao, X. (2013) How to prevent injury to the palmar cutaneous branch of median nerve and ulnar nerve in a palmar incision in carpal tunnel release, a cadaveric study. *Acta Neurochirurgica*, 155(9), 1751–1755.